Beam losses in the extraction line of a TeV e^+e^- linear collider with a 20 mrad crossing angle

A. Ferrari* and Y. Nosochkov†

22 December, 2005

Abstract

In this paper, we perform a detailed study of the power losses along the post-collision extraction line of a TeV e^+e^- collider with a crossing angle of 20 mrad between the beams at the interaction point. Five cases are considered here: four luminosity configurations for ILC and one for CLIC. For all of them, the strong beam-beam effects at the interaction point lead to an emittance growth for the outgoing beams, as well as to the production of beamstrahlung photons and e^+e^- pairs. The power losses along the 20 mrad extraction line, which are due to energy deposition by a fraction of the disrupted beam, of the beamstrahlung photons and of the e^+e^- coherent pairs, were estimated in the case of ideal collisions, as well as with a vertical position or angular offset at the interaction point.

*Uppsala University, Sweden
†Stanford Linear Accelerator Center, USA

Work supported in part by Department of Energy contract DE-AC02-76SF00515

1 Introduction

In a high-energy e^+e^- linear collider, the beams must be focused to extremely small spot sizes in order to achieve high charge densities and, in turn, to reach the desired luminosity. Because of the extremely small transverse dimensions of the colliding beams, electrons and positrons experience very strong transverse electromagnetic fields at the interaction point. The subsequent bending of their trajectories leads to the emission of hard beamstrahlung photons, which can then turn into e^+e^- (coherent and incoherent) pairs. Because of the large angular divergence and energy spread of the disrupted beams, a careful design of the extraction lines must be performed in order to transport the outgoing beams and the beamstrahlung photons from the interaction point to their dumps, with as small losses as possible. Also, the extraction lines should be fully instrumented to measure the main properties of the outgoing beams. In this study, we estimate the beam losses in the extraction line of a 1 TeV e^+e^- linear collider. This may correspond either to the early stages of the multi-TeV Compact Linear Collider (CLIC) or to an upgraded version of the International Linear Collider (ILC).

The CLIC project aims at multi-TeV e^+e^- collisions [1, 2]. In order to keep the length of the machine reasonably short, the design accelerating gradient and RF frequency are respectively 150 MV/m and 30 GHz. The bunch spacing is only a few cm, which is far too short to allow head-on collisions. At CLIC, the relative orientation of the linacs will be determined by the multi-TeV crossing angle [3]. For a center-of-mass energy of 3 TeV, the angular distribution of the e^+e^- coherent pairs is such that the crossing angle θ_c must be larger than 20 mrad to avoid activation of the last quadrupole of the incoming beam line. On the other hand, because of the crossing angle, synchrotron radiation is emitted by the incoming particles in the solenoid field, as well as in the final quadrupole of the incoming beam line, which leads to an increase of the spot size at the interaction point. However, this growth remains acceptable if $\theta_c \leq 20$ mrad. When combining the effects of the secondary background due to coherent pairs and of the luminosity loss due to synchrotron radiation, one finds that the optimal crossing angle for CLIC should be 20 mrad. In addition, with this value of θ_c one keeps the multi-bunch kick instabilities at an acceptable level (these instabilities are induced by the parasitic collisions between the incoming and outgoing bunches and they are enhanced by a vertical offset). When bunches are collided with a large crossing angle, a significant fraction of the luminosity can be lost. At CLIC, without further action, the luminosity would indeed be about 10 times smaller with $\theta_c = 20$ mrad than in the case of head-on collisions. Therefore, crab cavities must be used: by deflecting the head and the tail of each bunch in opposite horizontal directions upstream of the interaction point, they force the bunches to be perfectly aligned when they collide, which in turn allows to recover the luminosity.

The ILC project [4] aims at e^+e^- collisions with a center-of-mass energy from 500 GeV to 1 TeV. With the superconducting technology, one can not reach very high acceleration frequencies. Therefore, the spacing between two consecutive bunches (about 100 m) is so large that multi-bunch kick instabilities do not occur at ILC and one is not forced to

use a large crossing angle for the e^+e^- collisions. The main challenge with very small crossing angles is the extraction of the disrupted beam, which is achieved by sending the outgoing beam off-center in large superconducting quadrupoles or sextupoles. On the other hand, for large crossing angles, one must deal with technical difficulties such as, for instance, large crab-crossing corrections, as well as with other complications due to the passage of the beams through the solenoid field of the surrounding detector. Two configurations are currently being studied in the ILC design: one with a small crossing angle (2 mrad) and one with a large crossing angle (20 mrad). Here, we focus on the second case only.

This report is organized as follows. In Section 2, we review the incoming and outgoing beam distributions at the interaction point for various luminosity configurations of the 1 TeV ILC and for the low-energy version of CLIC at 1 TeV, in the case of ideal collisions. Then, in Section 3, we perform particle tracking in the post-collision extraction line presently considered for a TeV e^+e^- collider with a 20 mrad crossing angle and we make a detailed estimation of the beam losses. In Sections 4 and 5, the effect of vertical position and angular offsets at the interaction point are studied. Finally, some conclusions are given in Section 6.

2 Incoming and outgoing beam distributions at the interaction point

At e^+e^- linear colliders, the very strong beam-beam interactions generate a significant distorsion of the transverse and longitudinal beam distributions at the interaction point. Knowing the properties of the incoming beam, the disrupted beam distributions at the interaction point can be obtained with the GUINEA-PIG code [5].

Several machine configurations are being studied to reach the ILC luminosity goals [6, 7]. Here, for a center-of-mass energy of 1 TeV, we consider four sets of parameters. One is referred to as nominal and the three others (hl1, hl2 and hl3) correspond to various high luminosity configurations. As for CLIC, an optimization of the machine design at 1 TeV was recently performed, with the same beam delivery system as for the multi-TeV operation [8]. More details about the corresponding incoming beam distributions at a 1 TeV ILC or CLIC machine are given in Table 1.

The transverse distributions of the disrupted beams are shown in Figures 1-5, for all configurations of the 1 TeV e^+e^- linear collider. Note that the double-peak shape of the x'-distributions is characteristic for collisions with flat beams. The very strong beam-beam interactions lead to an increase of the rms size and/or the angular divergence of the colliding beams, and therefore to a significant emittance growth at the interaction point (in both transverse directions).

Configuration at 1 TeV	CLIC	ILC nominal	ILC hl1	ILC hl2	ILC hl3
Particles per bunch (10^{10})	0.256	2.0	2.0	2.4	2.0
Bunches per RF pulse	220	2820	2820	2820	2820
Bunch spacing (ns)	0.267	307.7	307.7	307.7	307.7
Beam current (A)	1.5	0.0104	0.0104	0.0125	0.0104
Repetition frequency (Hz)	150	4	4	4	4
Primary beam power (MW)	6.8	18.1	18.1	21.7	18.1
$(\beta\gamma)\epsilon_x$ in 10^{-6} m.rad	0.660	10	10	10	10
$(\beta\gamma)\epsilon_y$ in 10^{-6} m.rad	0.001	0.04	0.03	0.023	0.023
σ_x in nm	94	554	320	550	470
σ_y in nm	1.0	3.5	2.5	2.7	2.7
σ_z in μm	30.8	300	150	300	300
Luminosity (10^{34} cm^{-2} s^{-1})	2.8	2.8	7.8	5.7	4.6
Photons per e^+ or e^-	0.9	1.4	2.2	1.7	1.7
Beamstrahlung loss δ_B	9.0%	4.8%	17.6%	6.7%	6.5%

Table 1: Incoming beam parameters for various configurations of a 1 TeV e^+e^- linear collider (CLIC or ILC).

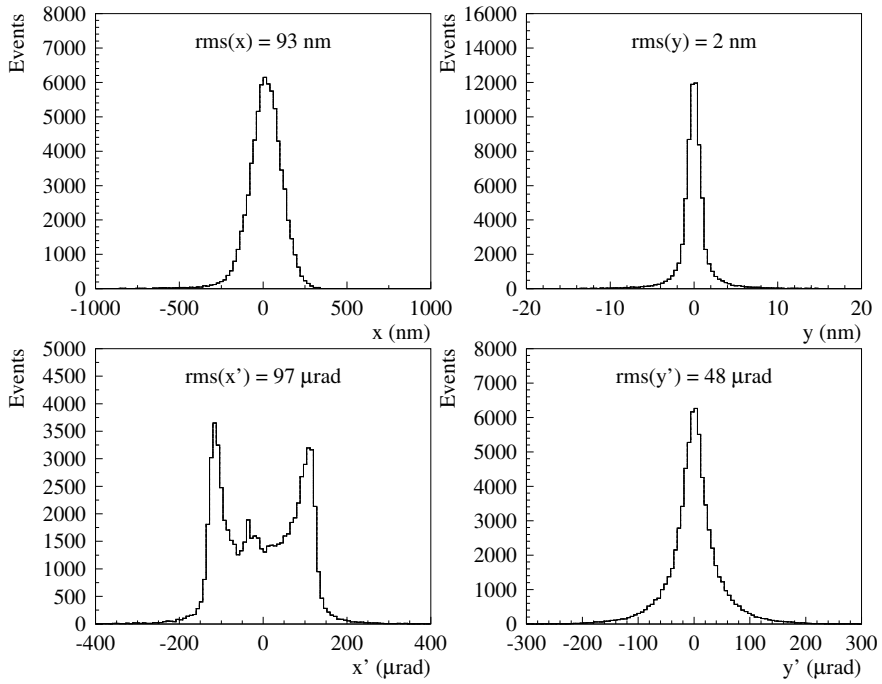

Figure 1: Transverse distributions of the disrupted beams at the interaction point of a 1 TeV CLIC machine.

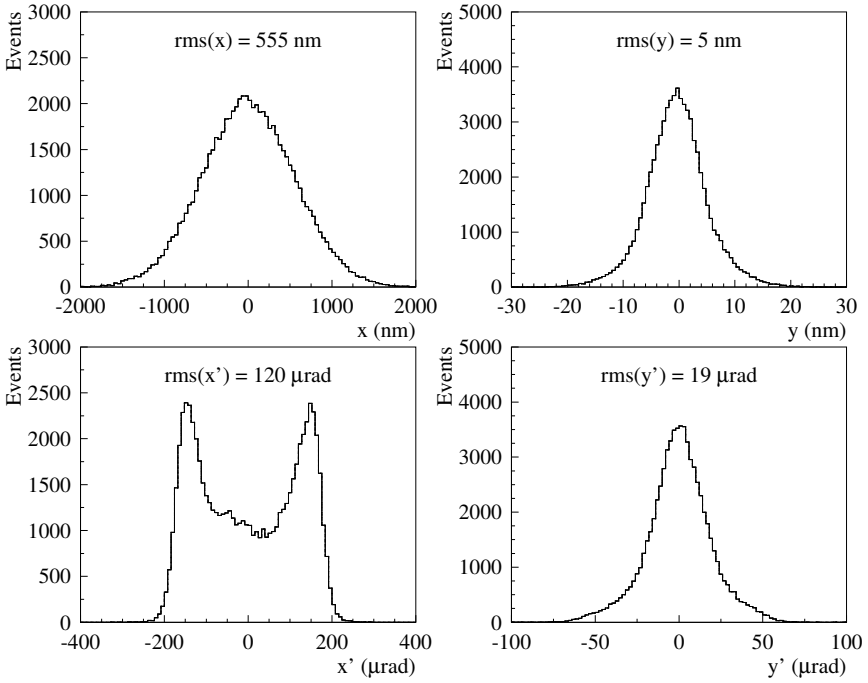

Figure 2: Transverse distributions of the disrupted beams at the interaction point of ILC, for a center-of-mass energy of 1 TeV, in the nominal configuration.

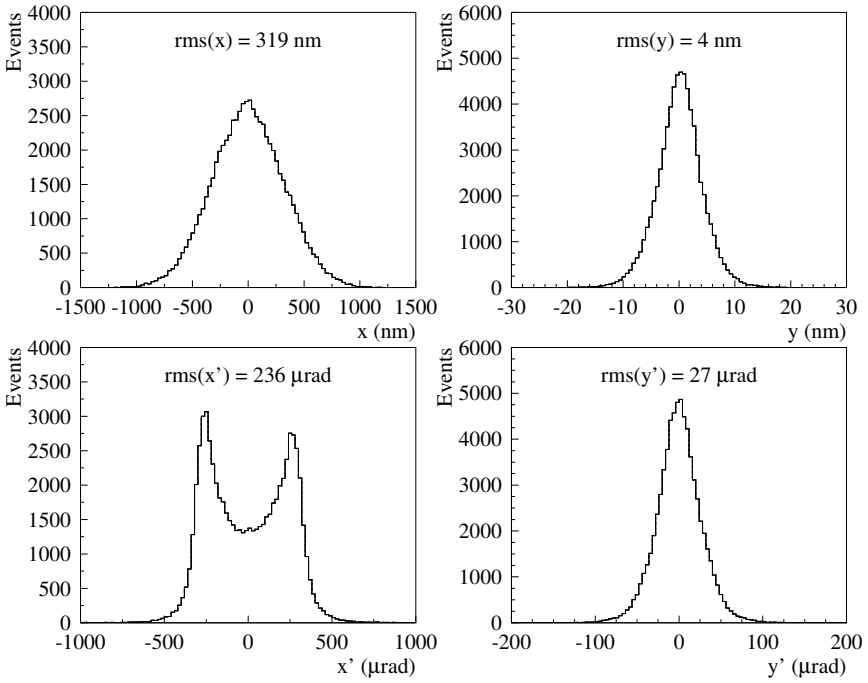

Figure 3: Same as Figure 2, in the high luminosity hl1 configuration.

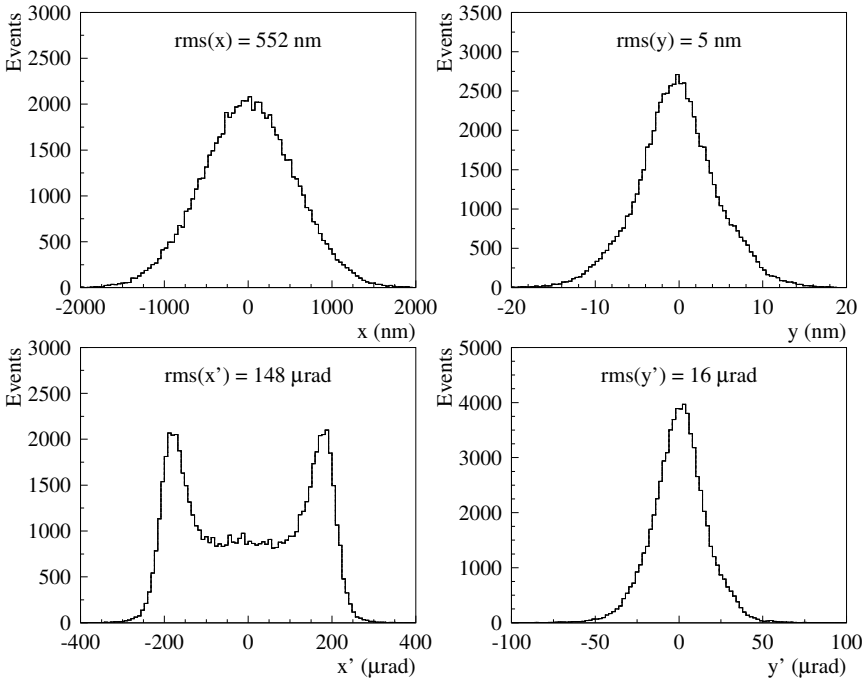

Figure 4: Same as Figure 3, in the hl2 configuration.

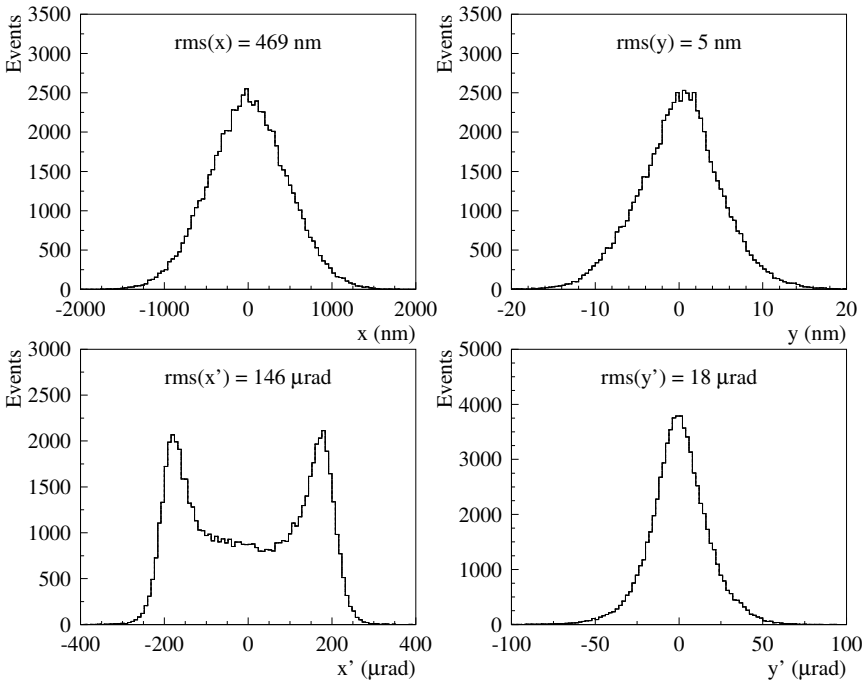

Figure 5: Same as Figure 3, in the hl3 configuration.

Figures 6 and 7 show the energy spectrum for the 1 TeV ILC, in the nominal and high luminosity configurations, and in the 1 TeV CLIC case, respectively. As the luminosity increases, the beam-beam interactions become stronger and stronger due to smaller transverse sizes of the incoming beams and, as a result, more and more beamstrahlung photons are emitted, leading to a larger energy spread and longer low-energy tails for the disrupted beams.

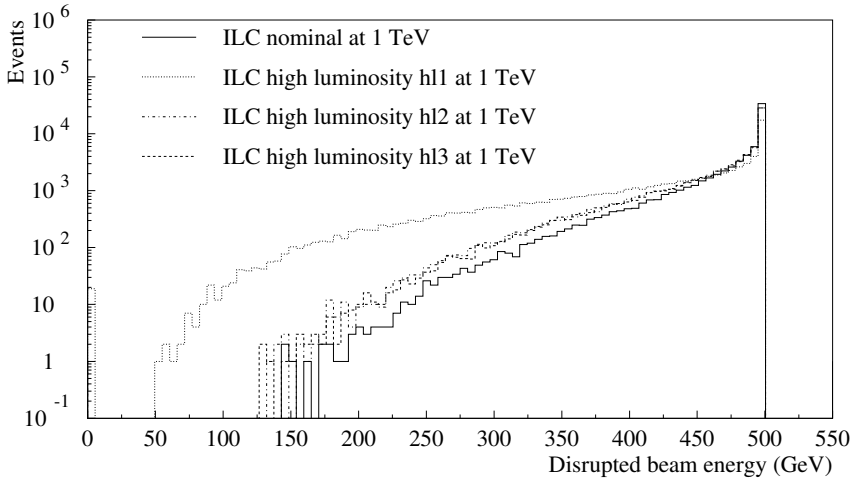

Figure 6: Energy spectrum of the disrupted beams at the ILC interaction point, for a center-of-mass energy of 1 TeV, in various configurations.

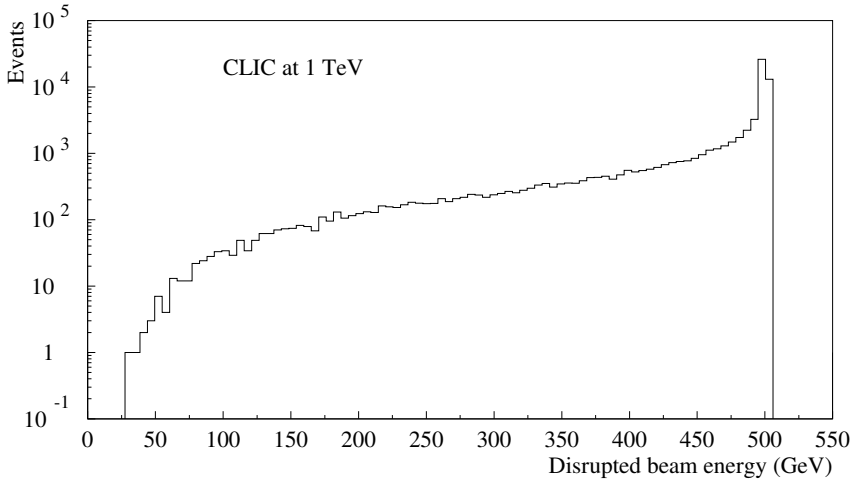

Figure 7: Same as Figure 6 in the case of a 1 TeV CLIC machine.

Note that, with the GUINEA-PIG program, one can produce data files not only for the disrupted beams themselves, but also for the beamstrahlung photons and the coherent or incoherent e^+e^- pairs. These secondary particles must also be transported to their dump with minimal losses.

3 Particle tracking in the extraction line

At an e^+e^- linear collider with a 20 mrad crossing angle, one will use a dedicated line to transport the outgoing beams (together with the beamstrahlung photons) from the interaction point to their dump. In the present design of the ILC 20 mrad extraction line [9], the disrupted beams and the beamstrahlung photons all go through the same magnets to one shared dump. The optics consists of a DFDF quadruplet, followed by two vertical chicanes for energy and polarization measurements and a field-free region that allows the beam to grow naturally, with two round collimators located 200 m and 300 m downstream of the interaction point, with a radius of 8.8 cm and 13.2 cm respectively, in order to reduce the maximum beam size at the dump.

Figure 8 shows the betatron functions and the vertical dispersion in the present design of the ILC post-collision line with a 20 mrad crossing angle. For this study, no dedicated design of a 20 mrad extraction line was performed in the case of CLIC at 1 TeV, and we thus consider exactly the same geometry and optics for both ILC and CLIC.

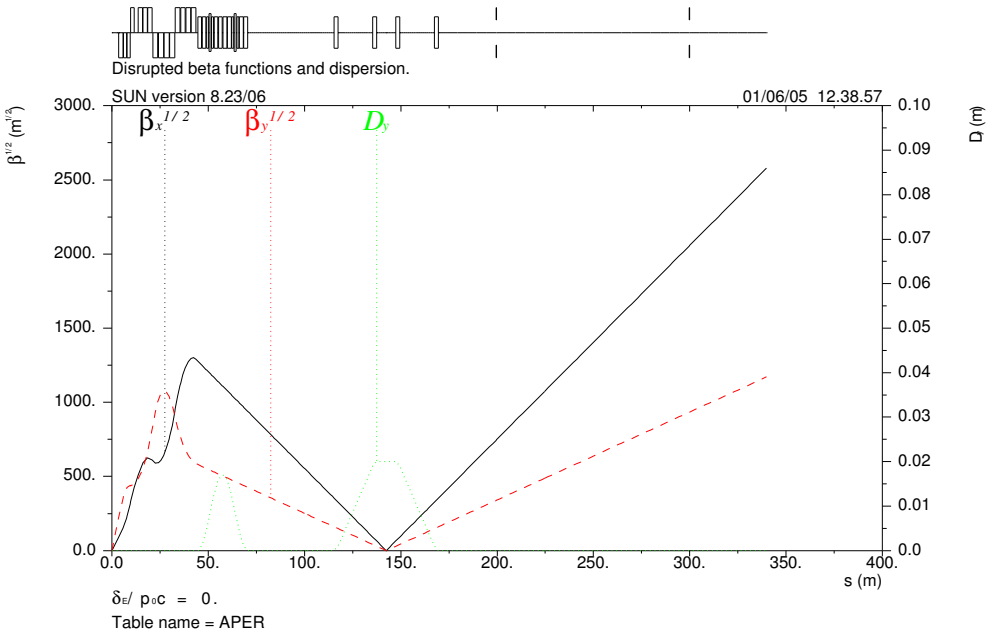

Figure 8: Betatron functions and vertical dispersion along the ILC extraction line with a 20 mrad crossing angle. This is an update of the lattice described in [9].

3.1 Power loss for the disrupted beams

The disrupted beam distributions of Figures 1-5 were tracked from the interaction point to the dump using DIMAD [10]. This program computes particle trajectories in a given beam line using the second order matrix formalism [11]. The DIMAD code was updated in order to handle very large energy spreads such as those found in the ILC or CLIC

disrupted beams downstream of the interaction point. Using the number of lost particles in the extraction line, as well as their energy, one can calculate the total beam power loss with the following formula:

$$P_{loss} = 1.602 \times 10^{-10} \, \frac{N_b \, n \, E \, f}{N_{tracks}} \, \sum_{i=1}^{N_{loss}} \left(1 + \frac{\delta E_i}{E} \right) . \qquad (1)$$

In this equation, N_b is the number of particles per bunch, n is the number of bunches per RF pulse, f is the repetition frequency (in Hz), E and $E_i = E + \delta E_i$ are respectively the nominal energy of the beam and the energy of the particle i (both in GeV), N_{tracks} and N_{lost} are respectively the number of tracked and lost particles. With these conventions, P_{loss} is expressed in Watts.

A comparison of the total power loss for the disrupted beams in the four ILC configurations considered in this study is shown in Figure 9.

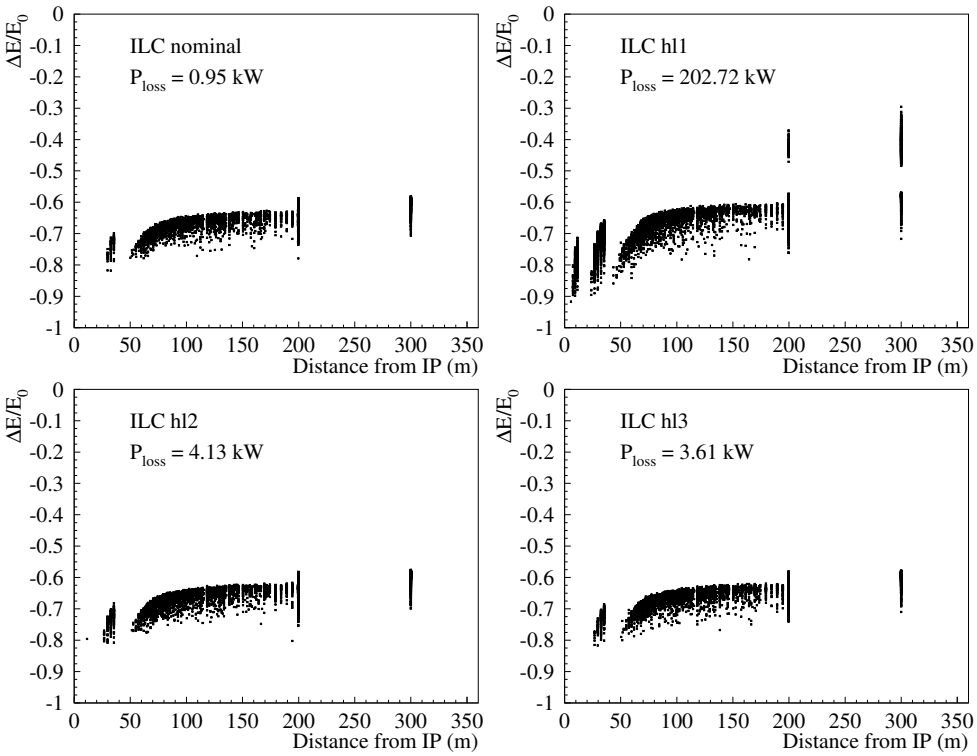

Figure 9: Relative energy spread of the lost particles as a function of the position of loss in the 20 mrad extraction for various ILC configurations (see Table 1 for details). A large amount of GUINEA-PIG e^+e^- events were produced in order to draw these plots (3.6×10^7 for ILC nominal, 1.7×10^5 for ILC hl1, 8.0×10^6 for ILC hl2, 9.6×10^6 for ILC hl3) so that about 10000 lost particles could be collected for further analysis in each ILC configuration.

This particle tracking with DIMAD clearly shows that most of the beam losses come from the low-energy tail. Indeed, the 20 mrad extraction line accepts most of the primary electrons/positrons with $E/E_0 > 40\%$, except in the hl1 case, where a few high-energy particles are lost in the round collimators. At the interaction point, those particles were exclusively found in the tails of the x'-distribution, namely they have $|x'| > 0.4$ mrad. In the other ILC configurations, the rms of the x'-distribution is small enough to ensure a full transmission of high-energy particles by the extraction line.

Note that the vertical line pattern in Figure 9 is due to the structure of the DIMAD output, where losses are assigned to each element of the beam line, instead of being continuously distributed. In order to better estimate the impact of the disrupted beam losses, Figure 10 shows the loss density in all elements of the 20 mrad extraction line, upstream of the collimators, for the four ILC configurations considered in our study.

For this first part of the extraction line, we have estimated the total beam losses and the largest value of the loss density in the superconducting and warm quadrupoles, as well as in the bending magnets of the energy and polarimetry chicanes, see Table 2.

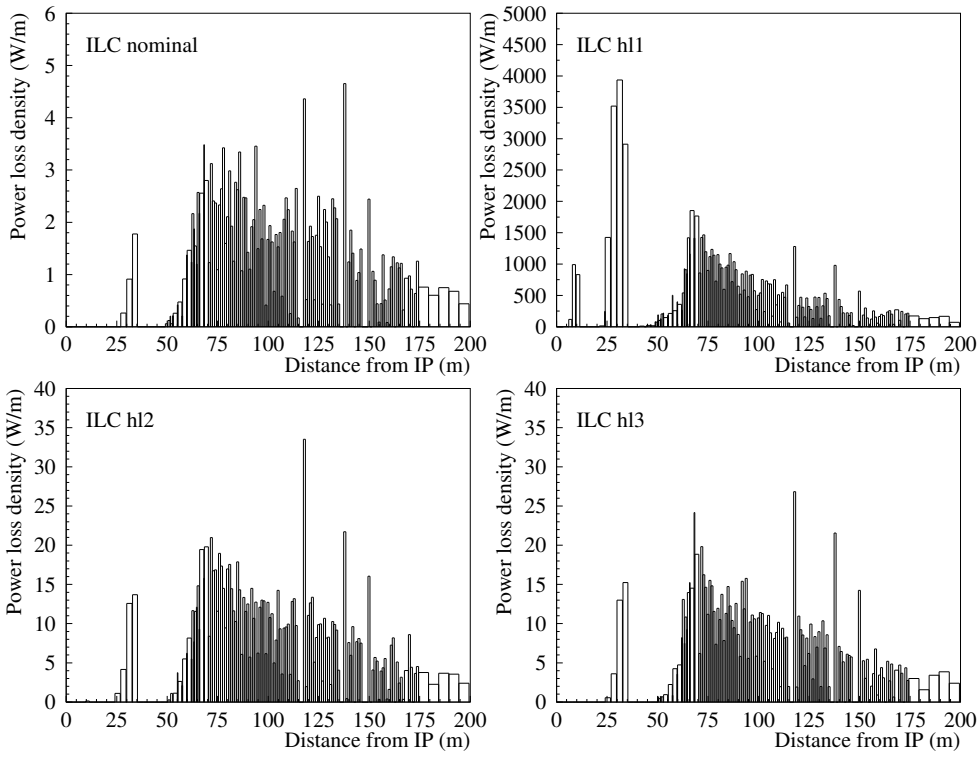

Figure 10: Loss density for the disrupted beams along the ILC 20 mrad extraction line, upstream of the collimators, for various ILC configurations at 1 TeV.

ILC configuration at 1 TeV	nominal	hl1	hl2	hl3
Total beam losses (W)				
SC Quadrupoles	0	3.2×10^3	0.2	0
Warm Quadrupoles	7.4	3.0×10^4	80.1	82.0
Energy Chicane Magnets	23.5	1.3×10^4	152.7	130.1
Polarimetry Chicane Magnets	1.8	5.4×10^2	8.0	8.2
Maximal loss density (W/m)				
SC Quadrupoles	0	1.0×10^3	0.1	0
Warm Quadrupoles	1.8	3.9×10^3	13.7	15.2
Energy Chicane Magnets	2.8	1.9×10^3	19.8	18.8
Polarimetry Chicane Magnets	0.9	2.7×10^2	4.0	4.1

Table 2: Total beam losses and maximal loss density in the first section of the 20 mrad extraction line (upstream of the collimators), for various ILC configurations at 1 TeV. About 10000 lost particles were used for this analysis.

With the nominal, hl2 and hl3 ILC configurations at 1 TeV, there is (almost) no beam loss in the four superconducting quadrupoles, i.e. along the first defocusing triplet and in the first quadrupole of the following (focusing) section. On the other hand, the hl1 configuration leads to loss densities up to 1 kW/m in the superconducting quadrupoles. As for the warm quadrupoles, in all ILC configurations, beam losses mostly occur in the last two quadrupoles of the third (defocusing) section and the first quadrupole of the last (focusing) section. In the energy chicane, the power loss in the bending magnets increases with the distance s to the interaction point along the chicane. Finally, in the polarimetry chicane, beam losses are concentrated in the last magnet.

As for the beam losses in the two round collimators (COLL1 and COLL2), we find:

- for ILC nominal: 0.6 kW in COLL1 and 0.1 kW in COLL2,
- for ILC hl1: 62.7 kW in COLL1 and 40.9 kW in COLL2,
- for ILC hl2: 2.5 kW in COLL1 and 0.4 kW in COLL2,
- for ILC hl3: 2.2 kW in COLL1 and 0.4 kW in COLL2.

The same study was performed by tracking the 1 TeV CLIC disrupted beam along the 20 mrad extraction line, see Figure 11. Here as well, most of the losses come from the low-energy tail, which has almost the same extension as in the ILC hl1 configuration (note however that, in the CLIC case, no high-energy particles are lost in the round collimators, thanks to a smaller rms value of the x'-distribution). For the first part of the extraction line, we have estimated the total beam losses and the largest value of the loss density in all magnetic elements, see Table 3. As for the beam losses in the two round collimators, we find 13.9 kW in COLL1 and 1.9 kW in COLL2.

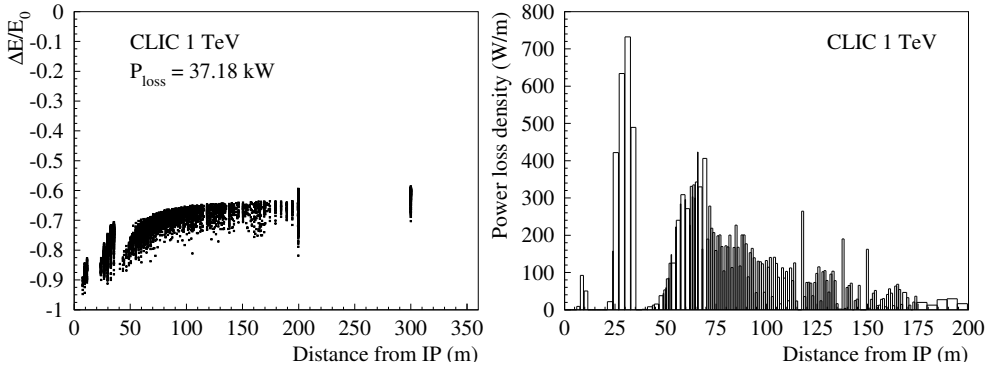

Figure 11: Relative energy spread of the lost particles as a function of the position of loss in the 20 mrad extraction line (left) and loss density upstream of the collimators (right), obtained when tracking the disrupted beam of the 1 TeV CLIC case. Here, 2.8×10^5 e^+e^- events were produced with GUINEA-PIG, in order to collect about 10000 lost particles for further analysis.

Magnetic elements	Total beam losses	Maximal loss density
SC Quadrupoles	0.25 kW	92.2 W/m
Warm Quadrupoles	5.96 kW	732.1 W/m
Energy Chicane Magnets	4.74 kW	406.0 W/m
Polarimetry Chicane Magnets	0.10 kW	46.4 W/m

Table 3: Total beam losses and maximal loss density in the first section of the 20 mrad extraction line (upstream of the collimators) for CLIC at 1 TeV. About 10000 lost particles were used for this analysis.

3.2 Power loss for the beamstrahlung photons

In addition to the significant growth of the emittance at the interaction point, strong beam-beam effects also lead to the emission of beamstrahlung photons by the colliding particles, with an associated power of a few MW. These photons must be transported to their dump with minimal losses along the extraction line.

Since photons do not carry any electric charge, they are not affected by magnetic fields and thus follow straight trajectories, which are fully determined by their initial angle at the interaction point. As a result, one can treat them exactly as electrons or positrons traveling through field free regions. It is possible to track beamstrahlung photons with DIMAD but, for this purpose, one assigns their original position to $x = y = 0$, switch-off all magnetic elements along the extraction line and turn-off charged particle effects, such as synchrotron radiation. In addition, when tracking photons, one must make sure that all magnets are placed on the reference trajectory, which is defined by the nominal

energy electron or positron beam. In other words, one needs to vertically misalign all elements inside the chicanes, so that the beamstrahlung photons go correctly through their aperture.

Using the number of lost photons in the extraction line, one then calculates the total beamstrahlung power loss with the following formula:

$$P_\gamma = 1.602 \times 10^{-10} \frac{N_\gamma \, n \, f}{N^\gamma_{tracks}} \sum_{i=1}^{N^\gamma_{loss}} E_{\gamma i}. \tag{2}$$

In this equation, N_γ is the number of beamstrahlung photons emitted by bunch crossing in a given direction (note that GUINEA-PIG produces photons along both outgoing beam directions) and $E_{\gamma i}$ is the energy of each lost photon.

Our simulations with DIMAD indicate that beamstrahlung photon losses occur almost exclusively in the first round collimator (and also in the second one, however in a much lesser extent). Located 200 m downstream of the interaction point, with a radius of 8.8 cm, COLL1 allows only beamstrahlung photons produced with an angle smaller than 0.44 mrad to pass through (this is chosen to limit the disrupted beam size to a 150 mm radius of the dump window). Thus, one critical parameter is the size of the beamstrahlung photon cone. For the CLIC machine and each ILC configuration, we calculated the rms value of the x'- and y'-distributions of the beamstrahlung photons obtained with GUINEA-PIG (for both outgoing beams), as well as the losses in COLL1 and COLL2. Table 4 shows that the larger the beamstrahlung photon cone, the larger the losses in the collimators. Note that, although the CLIC configuration has a smaller beamstrahlung photon cone than the ILC hl2 and hl3 cases, it leads to larger losses, because the emitted photons tend to carry more energy.

Configuration at 1 TeV	CLIC	ILC nominal	ILC hl1	ILC hl2	ILC hl3
Rms(x') in μrad	14.5	20.2	38.5	22.0	23.3
Rms(y') in μrad	15.3	12.8	18.6	11.7	10.6
Produced e^+e^- events	2.8×10^5	3.6×10^7	1.7×10^5	8.0×10^6	9.6×10^6
Beamstrahlung photons	5.1×10^5	1.1×10^8	7.8×10^5	2.7×10^7	3.3×10^7
Lost photons (total)	39	0	2403	23	12
Power loss COLL1 (W)	1.27	0	1201.80	0.06	0.02
Power loss COLL2 (W)	0	0	15.46	0	0

Table 4: Beamstrahlung photon cone sizes, amount of tracked/lost photons, and losses in the 20 mrad extraction line, for various configurations of a 1 TeV e^+e^- linear collider (CLIC or ILC). The amounts of generated e^+e^- events used in this analysis are the same as in the previous section.

Beamstrahlung photons lead to significant power losses in the ILC hl1 configuration only, where one has both long low-energy tails in the disrupted beams and a large horizontal photon cone size at the interaction point. Figure 12 shows the angular distributions of the beamstrahlung photons that are lost in the two round collimators.

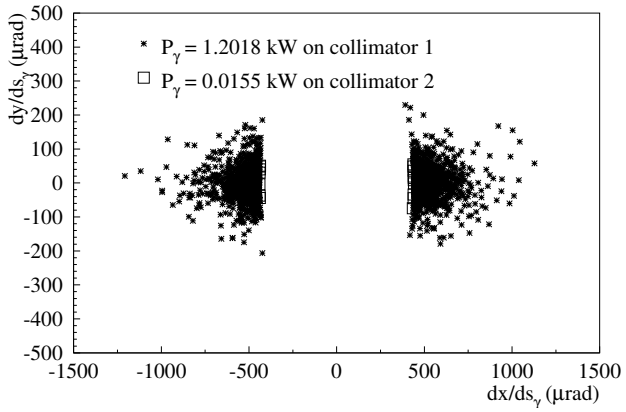

Figure 12: Angular x'- and y'-distributions of the beamstrahlung photons lost on the two round collimators of the 20 mrad extraction line, for the high luminosity hl1 ILC machine at 1 TeV.

3.3 Power loss for the coherent pairs

In the presence of a strong electromagnetic field, beamstrahlung photons can turn into e^+e^- coherent or incoherent pairs. The coherent pairs arise from the interaction of the beamstrahlung photons of one beam with the collective electromagnetic field of the other beam. The incoherent pairs result from the interaction of (real or virtual) photons of one beam with particles from the other beam. At 1 TeV, one expects about 10^5 to 10^6 incoherent pairs per bunch crossing. However, most of them have an energy smaller than 1 GeV and a polar angle extending almost up to 0.5 rad. The main concern with the e^+e^- incoherent pairs is how they contribute to the detector background [12], rather than the tiny amount of power deposited by a fraction of these low-energy pairs in the extraction line. In the following, we thus only focus on the e^+e^- coherent pairs, which carry significantly more energy.

The probability associated to the e^+e^- coherent pair production depends essentially on the beamstrahlung parameter Υ defined as:

$$\Upsilon = \frac{5}{6}\,\frac{\gamma r_e^2 N_b}{\alpha\sigma_z\sigma_x(1+\sigma_x/\sigma_y)}, \tag{3}$$

where $\alpha = 1/137$ and $r_e = 2.82 \times 10^{-15}$ m are respectively the fine-structure constant and the classical electron radius.

When Υ is smaller than unity, the number of coherent pairs per incoming electron or positron increases exponentially with Υ [13]. As a result, it can be shown that, with a few 10^{10} particles per bunch, the e^+e^- coherent pair production remains negligible as long as the beamstrahlung parameter Υ remains smaller than 0.2. This is the case at a 1 TeV ILC machine, in the nominal, hl2 and hl3 configurations (where one has $\Upsilon \simeq 0.1$). On the other hand, for the hl1 configuration ($\Upsilon = 0.37$), one expects 3.6×10^5 coherent pairs per bunch crossing. Finally, at the 1 TeV CLIC machine, one has $\Upsilon = 0.78$ and the expected number of e^+e^- coherent pairs is 5.3×10^5 per bunch crossing. Both for the ILC hl1 configuration and for CLIC, the amount of coherent pairs was estimated with GUINEA-PIG simulations. The electrons and positrons of such pairs carry typically about 10% of the primary beam energy, i.e up to 50 GeV.

We first consider the CLIC machine at 1 TeV, which has the largest number of coherent pairs per bunch crossing. About 2.8×10^6 e^+e^- collisions were generated with GUINEA-PIG in order to study the losses due to coherent pairs in the 20 mrad extraction line with enough statistics. For a given disrupted beam direction, one must run two tracking simulations with DIMAD: one for the particles that have the same charge as the disrupted beam and one for the particles with the opposite charge. In the latter case, since DIMAD does not know the charge of the particle that is tracked, one needs to change the polarity of all magnetic elements and, in addition, one must make sure that all magnets are placed on the reference trajectory defined by the nominal (undisrupted) beam. For this purpose, one must vertically misalign all elements inside the chicanes, so that the wrong-sign particles go correctly through them. However, the corresponding reduction of aperture remains of the order of a few percent only and thus does not significantly affect the losses.

About 75% of the particles coming from the coherent pairs do not reach the dump at the end of the extraction line. The left-hand side plot of Figure 13 shows that losses mostly occur due to over-focusing of low-energy particles in the quadrupoles: indeed, the lower the energy of the tracked particle, the sooner it is lost after the interaction point. This plot also indicates that the distribution of the power losses along the extraction line does not significantly depend on the particle charge. As for the right-hand side plot of Figure 13, it shows that the power loss density (estimated for both electrons and positrons) remains at a reasonable level, a few W/m only, which is negligible compared to the power loss density of the disrupted beam. One can thus forget the contribution of e^+e^- coherent pairs to the beam losses at a 1 TeV CLIC machine.

The amount of coherent pairs produced in e^+e^- collisions at ILC for a center-of-mass energy of 1 TeV remains negligible for all configurations, except hl1. Still, in that latter case, one expects these low-energy electrons and positrons to be even less numerous than at the 1 TeV CLIC machine. One can therefore neglect their contribution to the beam losses in the 20 mrad extraction line.

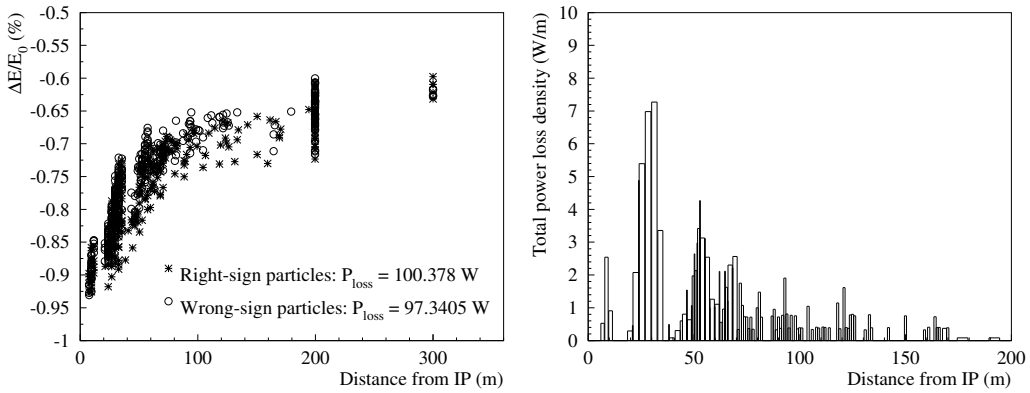

Figure 13: Relative energy spread of the lost particles as a function of the position of loss in the 20 mrad extraction line (left) and power loss density upstream of the collimators, obtained by tracking e^+e^- coherent pairs, in the 1 TeV CLIC case. Here, 2.8×10^6 events were produced with GUINEA-PIG, in order to collect about 900 lost particles for further analysis.

4 Effects of a vertical position beam-to-beam offset at the interaction point

Having studying in detail beam losses in the case of ideal e^+e^- collisions, let us now introduce a vertical position offset at the interaction point, which can occur during initial tuning. This may increase the vertical angular divergence of the disrupted beam and lead to larger losses in the extraction line [14].

4.1 Disrupted beams, beamstrahlung photons and coherent pairs with a vertical position offset

When the incoming electron and positron beams are vertically flat, like at ILC or CLIC, horizontal position offsets do not really affect the disruption process at the interaction point and the beam losses in the extraction line downstream. On the other hand, the beam-beam effects may increase significantly when a vertical offset is introduced. For relatively small offsets, the electromagnetic field seen by the bulk of charged particles in one beam increases with the distance to the other beam, and so does the disruption and, in turn, the emission of beamstrahlung photons. For larger offsets, the field seen by each bunch becomes smaller and smaller as the distance between the incoming beams increases: at very large offsets, the disrupted beam distributions eventually converge to the incoming beam distributions and the beamstrahlung photon emission disappears. The disrupted beam parameters and the angular distributions of the beamstrahlung photons obtained with a vertical position offset were studied with GUINEA-PIG for the five CLIC/ILC configurations at 1 TeV, see Figures 14 and 15 for details.

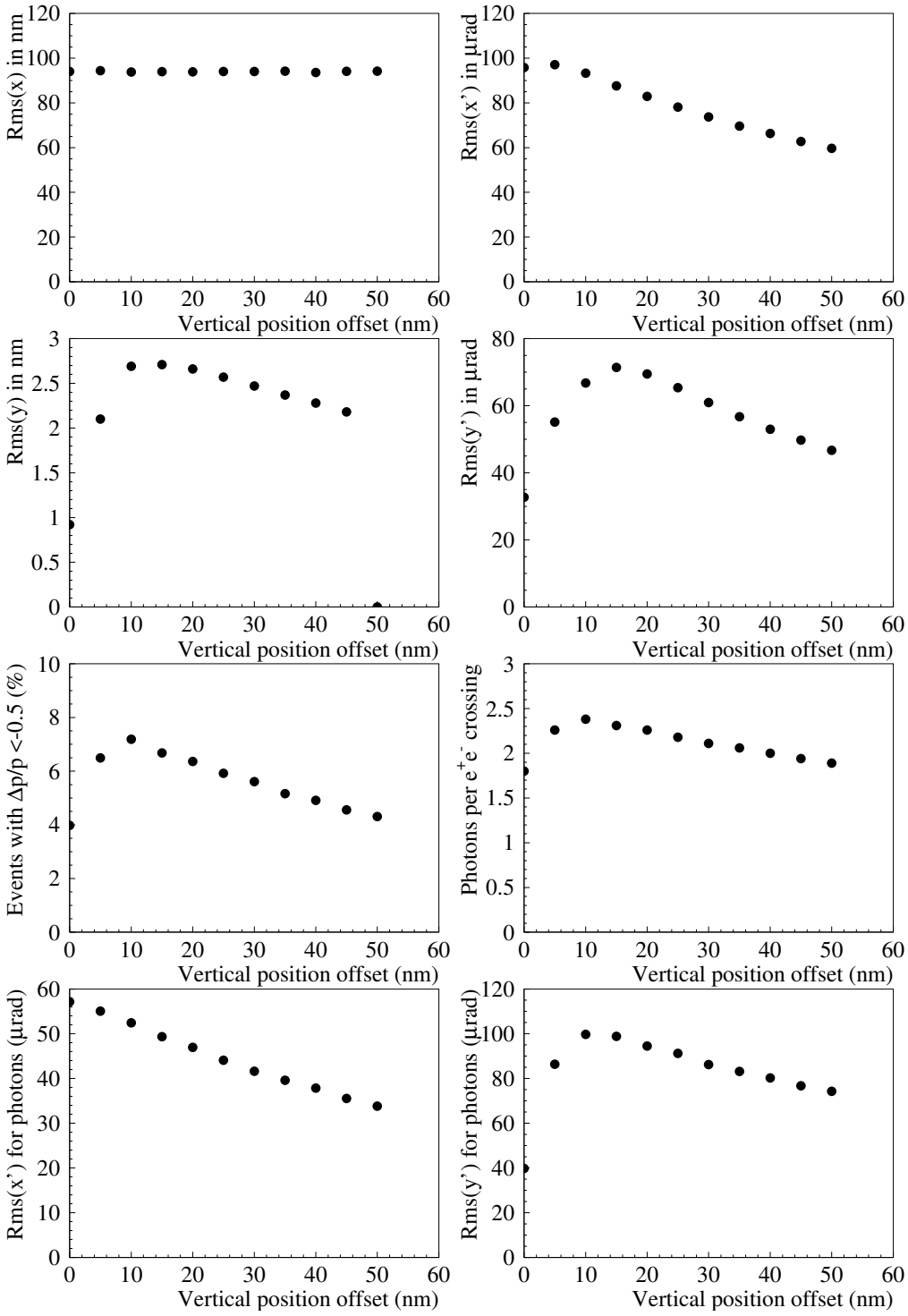

Figure 14: Main characteristics of the disrupted beam and the beamstrahlung photons at the interaction point, as a function of the vertical position offset at a 1 TeV CLIC machine.

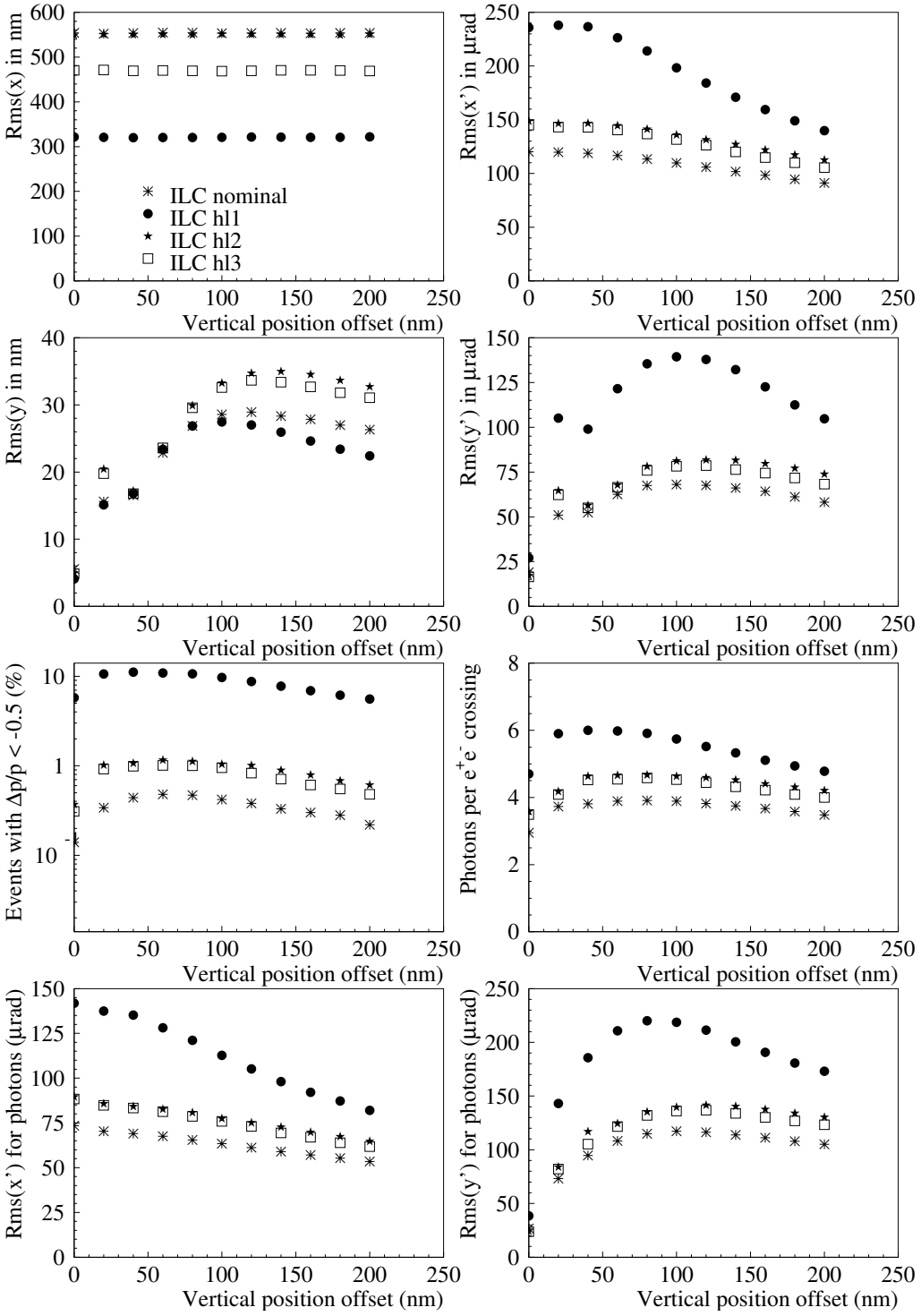

Figure 15: Main characteristics of the disrupted beam and the beamstrahlung photons at the interaction point, as a function of the vertical position offset, for various ILC configurations at 1 TeV.

Our simulations indicate that beam-beam effects become maximal for an offset Δy of 10 to 30 σ_y. A blow-up of the emittance clearly occurs. Also, there are between two and three times more particles with $\Delta p/p < -0.5$ in the e^+ and e^- bunches, which are then likely to be lost in the extraction line. In addition, note that more beamstrahlung photons are produced and that their vertical angular distribution is much wider than without vertical offset. On the other hand, the horizontal angular distributions of both the disrupted beam and the beamstrahlung photons become more and more narrow when the vertical offset increases. At CLIC and in the ILC hl1 configuration, the number of coherent pairs per bunch crossing is about 5 to 6 times larger when Δy reaches 10 to 30 σ_y than when there is no vertical offset. However, as already pointed out, their contribution to the losses along the extraction line is negligible.

4.2 Power loss in the extraction line with a vertical position offset

As a result of the increased emittance and energy spread that are induced by a vertical position offset, one can expect larger losses for the disrupted beams along the 20 mrad extraction line, as illustrated by Figure 16.

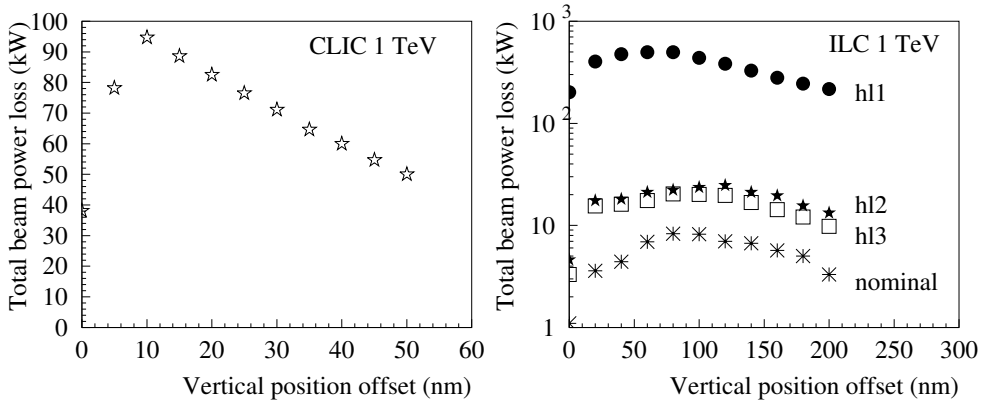

Figure 16: Disrupted beam power losses in the extraction line as a function of Δy, for CLIC (left) and various ILC configurations (right) at 1 TeV.

A detailed analysis of the power loss distribution along the 20 mrad extraction line was performed with the vertical position offset leading to the largest disrupted beam losses, see Table 5. A comparison with Tables 2 and 3 shows that these losses may increase by a factor 2 to 4 in the quadrupole sections, without significant differences between the five cases that are studied here. On the other hand, the energy deposition in the magnetic chicanes and the collimators strongly depends on the 1 TeV configuration that one considers. In these sections of the extraction line, which have a non-zero (nominal or residual) dispersion, a larger relative increase of the beam energy spread due to the vertical offset leads to significantly more power losses. Note that, in the ILC hl1 case, the power loss in the second round collimator is smaller with a vertical position offset

than without. Since the x'-distribution at the interaction point becomes more and more narrow as the vertical offset increases, the few high-energy particles with $|x'| > 440$ μrad, which can hit the collimators when there is no vertical offset, now have a sufficiently small x' to reach the dump.

Configuration at 1 TeV	CLIC	ILC nominal	ILC hl1	ILC hl2	ILC hl3
	Vertical offset for maximal losses				
Δy_{max} expressed in σ_y	10	23	24	44	33
	Total disrupted beam losses (kW)				
SC Quadrupoles	0.49	0	4.99	0	0
Warm Quadrupoles	15.50	0.02	64.88	0.35	0.17
Energy Chicane Magnets	22.42	0.87	93.67	4.12	1.96
Polarimetry Chicane Magnets	0.36	0.03	1.26	0.10	0.13
Round collimator COLL1	30.75	5.03	150.34	13.67	12.06
Round collimator COLL2	2.84	0.83	70.66	1.08	1.24
Along the extraction line	94.73	8.33	498.35	24.67	20.40

Table 5: Disrupted beam losses in various sections of the 20 mrad extraction line, as obtained when Δy is set to the value that maximizes the power loss.

Beamstrahlung photons only lead to significant power losses in the ILC hl1 configuration (at CLIC for instance, the power loss due to beamstrahlung photons on the collimators is maximal when $\Delta y = 15\,\sigma_y$, but it still remains smaller than 0.1 kW). Figure 17 shows how the beamstrahlung photon losses vary with Δy in the ILC hl1 configuration.

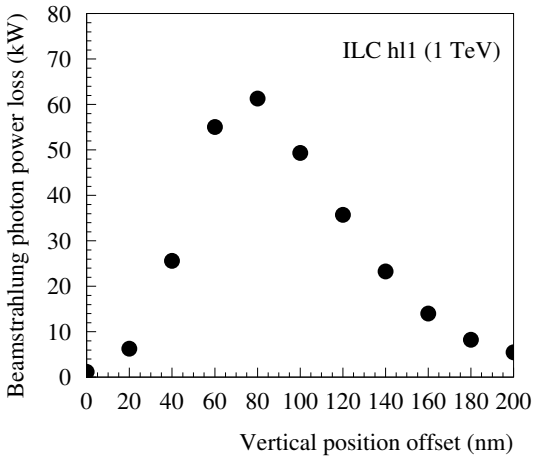

Figure 17: Power loss for the beamstrahlung photons as a function of the vertical position offset, for the ILC hl1 configurations at 1 TeV.

The maximal losses are obtained for $\Delta y \simeq 32\,\sigma_y$. For the small values of Δy, losses mostly occur because of the beamstrahlung photons with $|x'| > 440$ μrad. However, as Δy becomes larger, the photon cone shrinks in the horizontal direction and expands in the vertical direction. At large Δy values, the losses thus mostly occur because of the beamstrahlung photons that have $|y'| > 440$ μrad.

5 Effects of an angular offset at the interaction point

Having studied in detail the effects of a transverse position offset on the outgoing beam distributions and the subsequent losses along the post-collision extraction line, let us now consider an angular offset at the interaction point. When the colliding beams are vertically flat, they are not significantly affected by horizontal angular offsets. Actually, we noticed that the larger $\Delta x'$, the smaller both the luminosity and the power losses in the extraction line due to beam-beam effects at the interaction point. In the following, we therefore only focus on the effects of a vertical angular offset $\Delta y'$. Figure 18 shows the variation of the beam-beam effects with $\Delta y'$.

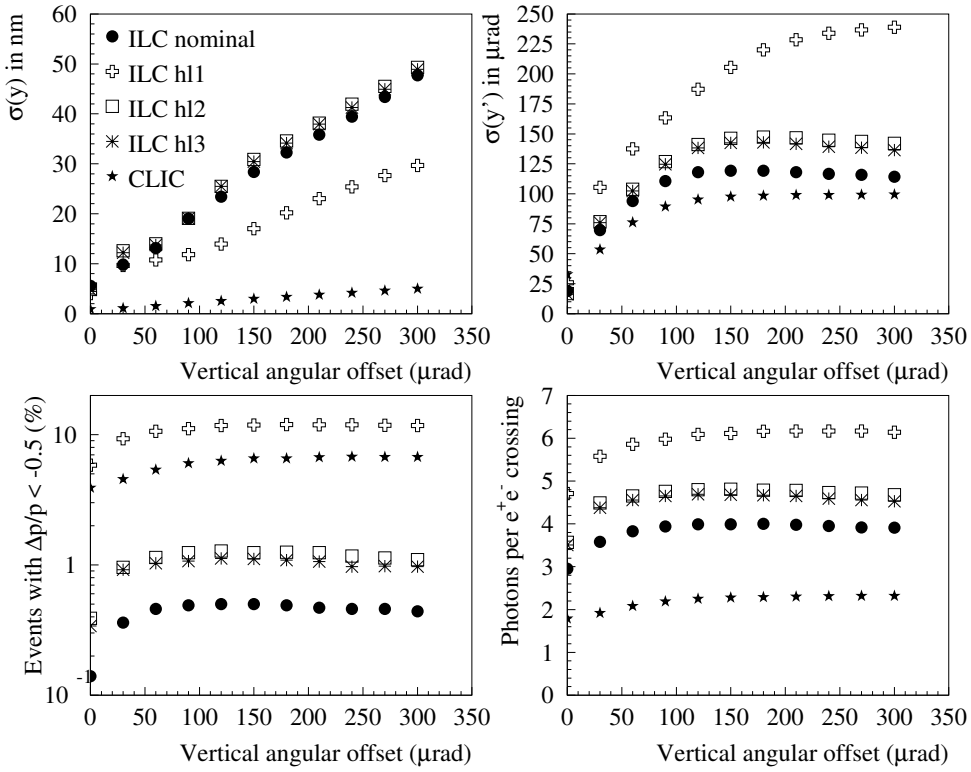

Figure 18: Disrupted beam vertical distributions, fraction of events with $\Delta p/p \leq -0.5$ and number of beamstrahlung photons per e^+e^- collision, as a function of the vertical angular offset for five different configurations of a TeV linear collider.

For all configurations considered for CLIC or ILC at 1 TeV, one observes a constant increase of the vertical rms size of the outgoing beam with the vertical angular offset, as well as a saturation of the beam-beam effects at $\Delta y' \simeq 100 - 200$ μrad.

The total power loss deposited by the disrupted beam along the 20 mrad extraction line depends on the vertical angular offset in roughly the same way as the beam-beam effects, as shown in Figure 19.

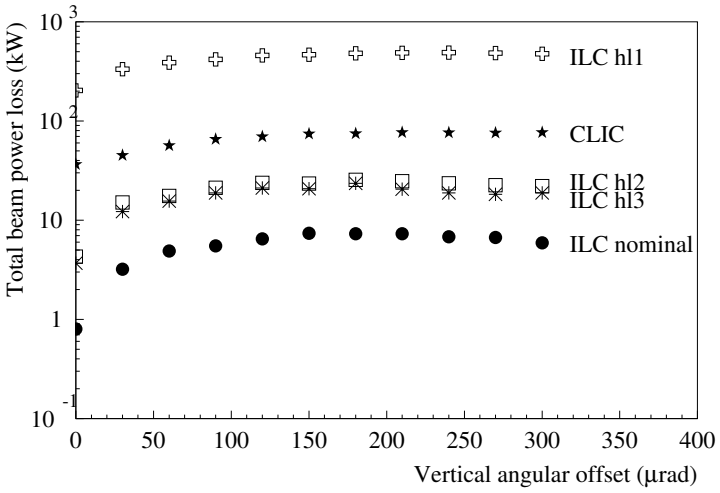

Figure 19: Total power losses in the 20 mrad extraction line, as a function of the vertical angular offset $\Delta y'$, for five different configurations of a TeV linear collider.

A detailed analysis of the loss distribution along the extraction line was performed with $\Delta y' = 300$ μrad, see Table 6. The maximal losses due to the vertical angular offset are slightly lower or comparable to the maximal losses due to the vertical position offset.

Configuration at 1 TeV	CLIC	ILC nominal	ILC hl1	ILC hl2	ILC hl3
	Total disrupted beam losses (kW), $\Delta y' = 300$ μrad				
SC Quadrupoles	0.52	0	5.67	0	0
Warm Quadrupoles	13.22	0.02	80.65	0.64	0.18
Energy Chicane Magnets	15.41	0.44	86.40	2.52	2.29
Polarimetry Chicane Magnets	0	0.26	1.27	0.06	0.13
Round collimator COLL1	25.60	4.00	143.98	12.54	10.65
Round collimator COLL2	2.71	0.29	44.94	1.08	1.54
Along the extraction line	76.82	5.93	476.33	22.06	18.80

Table 6: Total disrupted beam losses in the various section of the 20 mrad extraction line, for five different configurations of a TeV linear collider, with $\Delta y' = 300$ μrad.

In the ILC hl1 configuration, beamstrahlung photons should also be taken into account when estimating the power losses in the extraction line. With a non-zero vertical angular offset at the interaction point, tails appear in the upper part of the beamstrahlung photon y'-distribution (while the x'-distribution remains unaffected), see the left-hand side plot of Figure 20. This effect, together with an increased number of beamstrahlung photons per e^+e^- collision, lead to additional power losses (mostly on the collimators), as shown in the right-hand side plot of Figure 20. Here, the maximal losses due to the vertical angular offset are about twice smaller than the maximal losses due to the vertical position offset.

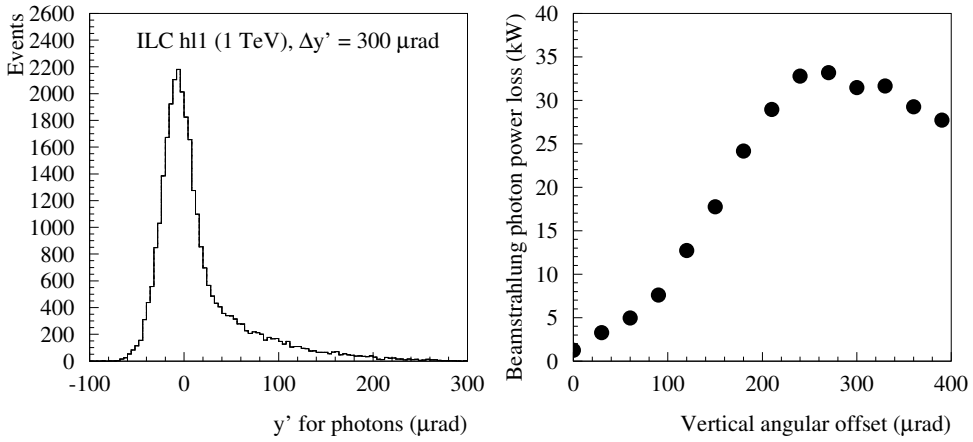

Figure 20: Beamstrahlung photon y'-distribution obtained with a vertical angular offset of 300 μrad (left) and beamstrahlung photon power losses in the extraction line as a function of $\Delta y'$ (right), for the ILC hl1 configuration at 1 TeV.

6 Conclusion

In this paper, a detailed study of the beam losses along the 20 mrad extraction line of a TeV e^+e^- collider was performed, for various CLIC or ILC configurations. In such high luminosity machines, very strong beam-beam interactions lead to an increase of the rms size and of the angular divergence of the colliding beams, especially in the vertical direction, and therefore to a significant emittance growth at the interaction point. In addition, strong beam-beam effects also lead to the emission of beamstrahlung photons by the colliding particles, with an associated power of a few MW. In the presence of a very strong electromagnetic field, these hard beamstrahlung photons can then turn into e^+e^- coherent pairs. All these particles must be transported with minimal power losses from the interaction point to their dump, through a post-collision extraction line.

For each ILC or CLIC configuration, we first performed a detailed study of the power losses along this extraction line in the case of ideal collisions. More than 99% of these losses are due to the disrupted beams. Beamstrahlung photons lead to significant losses only in the ILC hl1 configuration, which has the highest luminosity. In all cases, the power deposited by e^+e^- coherent pairs can be neglected. In the 1 TeV ILC nominal configuration, the power losses are about 1 kW and their distribution along the 20 mrad extraction line appears acceptable. The recently proposed ILC high luminosity hl2 and hl3 configurations should also allow to keep the power losses at a reasonable level in the extraction line, although these are 3 to 5 times larger than in the ILC nominal case. On the other hand, the beam losses become too large for the ILC high luminosity hl1 and CLIC configurations, with deposited power of respectively 36 kW and 201 kW along the extraction line.

The power losses in the 20 mrad extraction beam line were also studied as a function of a vertical position or angular offset at the interaction point (since the colliding beams are vertically flat, they are not significantly affected by horizontal offsets). It was found that the strongest beam-beam effects, and in turn the maximal power losses, occur when the vertical position offset is 10 to 30 σ_y or when the vertical angular offset reaches about 200 μrad.

This study allows validation of the presently considered design for the extraction beam line in the nominal and two newly proposed high luminosity hl2 and hl3 configurations of ILC. As for a 1 TeV CLIC machine and the ILC high luminosity hl1 configuration, another design should be investigated with smaller power losses. In addition, further studies of the beam losses along the extraction line should include a more detailed design of the magnetic elements and possibly additional collimators aimed at reducing the loss densities. Finally, it should be pointed out that DIMAD does not simulate the interactions between the lost particles and matter. A program called BDSIM [15] is presently under development in order to treat such secondary effects and estimate their impact on the losses in the extraction beam line. In addition, it should allow a more accurate estimation of the power loss densities because, in contrary to DIMAD that can only determine in which element a particle is lost, BDSIM can measure exact loss positions.

Acknowledgements

This work is supported by the Commission of the European Communities under the 6^{th} Framework Programme "Structuring the European Research Area", contract number RIDS-011899.

The authors wish to thank A. Seryi (SLAC), as well as D. Schulte (CERN), for very helpful discussions.

References

[1] The CLIC Study Team, ed. G. Guignard, "A 3 TeV e^+e^- linear collider based on CLIC technology", CERN 2000-008.

[2] I. Wilson, "The compact linear collider CLIC", CLIC note 617, CERN-AB-2004-100, published in Phys. Rep. 403-404 (2004) 365-378.

[3] D. Schulte and F. Zimmermann, "The crossing angle in CLIC", CLIC note 484, CERN-SL-2001-043 (AP), CERN-PS-2001-038 (AE), presented at the 2001 Particle Accelerator Conference, Chicago, USA, June 18-22, 2001.

[4] http://www.interactions.org/linearcollider/

[5] D. Schulte, TESLA-97-08 (1996).

[6] T. Raubenheimer, "Suggested ILC Beam Parameter Range", February 28th, 2005 (www-project.slac.stanford.edu/ilc/acceldev/beamparameters.html).

[7] A. Seryi, "Alternative 1 TeV high luminosity parameters", July 26th, 2005 (www-project.slac.stanford.edu/lc/bdir/Meetings/beamdelivery/2005-07-26/index.htm)

[8] F. Tecker *et al.*, CLIC note 627 in preparation.

[9] R. Arnold, K. Moffeit, Y. Nosochkov, W. Oliver, A. Seryi, E. Torrence and M. Woods, "Design of ILC extraction line for 20 mrad crossing angle", Proceedings of PAC 2005, Knoxville, USA.

[10] http://www.slac.stanford.edu/accel/ilc/codes/dimad

[11] K.L. Brown, D.C. Carey, Ch. Iselin and F. Rothacker, "TRANSPORT, a computer program for designing charged particle beam transport systems", SLAC 91, NAL 91 and CERN 80-04.

[12] C. Rimbault, P. Bambade, K. Mönig and D. Schulte, "Study of incoherent pair generation in Guinea-Pig", EUROTeV-Report-2005-016-1.

[13] P. Chen, "Coherent Pair Creation from Beam-Beam Interaction", SLAC-PUB 5086 (1989).

[14] Y. Nosochkov, T.O. Raubenheimer and K.A. Thompson, "NLC Beam Properties and Extraction Line Performance with Beam Offset at IP", SLAC-PUB 8872 (2001).

[15] G.A. Blair, "Simulation of the CLIC Beam Delivery System using BDSIM", CLIC note 509 (2002).